FABAD J. Pharm. Sci., 51, 1, 175-188, 2026
Doi: 10.55262/fabadeczacilik.1777903
RESEARCH ARTICLE

Dornase Alfa as a Potential Treatment Option for SARS-CoV-2: *In Vitro* Insights

Derya DİLEK KANÇAĞI[*°], Cihan TAŞTAN[**], Kevser Buse KARADENİZ[***], Selen ABANUZ[****], Didem ÇAKIRSOY[*****], Yaren BÜYÜKÇOLAK[******], Sezer AKYÖNEY[*******], Gözde SIR KARAKUŞ[********], Bulut YURTSEVER[*********], Koray YALÇIN[**********], İsmail Tuncer DEĞİM[**********], Ercüment OVALI[***********]

Dornase Alfa as a Potential Treatment Option for SARS-CoV-2: In Vitro Insights

SUMMARY

The potential use of dornase alfa (DA) in severe acute respiratory syndrome coronavirus 2 (SARS-CoV-2) infection has been widely discussed, yet its mechanisms remain insufficiently characterized. Here, we investigated whether DA modulates SARS-CoV-2 through multiple in vitro readouts, including viral infectivity, viral RNA integrity, spike-mediated entry, T-helper cytokine polarization, and neutrophil extracellular trap (NET) formation. DA at 30 U reduced viral infectivity ($p < 0.05$). Quantum dot–based quantitative flow cytometry showed that DA (10 U and 30 U) decreased viral internalization, consistent with spike-binding–mediated entry inhibition ($p < 0.05$). qRT-PCR and sequencing suggested altered integrity/fragmentation of naked viral RNA after exposure to 30 U DA ($p < 0.05$). Cytokine bead array analyses of viral peptide–stimulated lymphocytes indicated a shift toward a Th2-skewed response in the presence of DA ($p < 0.05$). In addition, fluorescence microscopy demonstrated that 30 U DA suppressed phorbol myristate acetate–induced NETosis in polymorphonuclear leukocytes. Overall, these findings provide preliminary, hypothesis-generating evidence that DA may modulate SARS-CoV-2–related responses via multiple mechanisms. Larger, adequately powered studies are needed to validate these findings. However, clinical efficacy and any potential prophylactic role require confirmation in appropriately designed in vivo and patient-based studies.

Keywords: *Coronavirus disease 2019, severe acute respiratory syndrome coronavirus 2, dornase alfa, neutrophil extracellular traps.*

Dornaz Alfa'nın SARS-CoV-2 İçin Potansiyel Bir Tedavi Seçeneği Olarak Kullanımı: İn Vitro Bulgular

ÖZ

Dornaz alfa'nın (DA) şiddetli akut solunum sendromu koronavirüs 2 (SARS-CoV-2) enfeksiyonunda potansiyel kullanımı yaygın biçimde tartışılmakla birlikte, etki mekanizmaları yeterince aydınlatılmamıştır. Bu çalışmada DA'nın, viral enfektivite, viral RNA bütünlüğü, spike aracılı giriş, T-helper sitokin polarizasyonu ve nötrofil ekstrasellüler tuzak (NET) oluşumu gibi çoklu in vitro çıktılar üzerinden SARS-CoV-2'yi modüle edip etmediği araştırılmıştır. DA'nın 30 U dozunda viral enfektiviteyi azalttığı gösterilmiştir ($p < 0,05$). Kuantum nokta (quantum dot) tabanlı kantitatif akım sitometrisi, DA'nın (10 U ve 30 U) viral internalizasyonu azalttığını ve bunun spike proteinine bağlanma aracılı giriş inhibisyonu ile uyumlu olduğunu göstermiştir ($p < 0,05$). qRT-PCR ve sekanslama analizleri, 30 U DA maruziyeti sonrası "çıplak" viral RNA'nın bütünlüğünde/parçalanma düzeyinde olası bir değişime işaret etmiştir ($p < 0,05$). Viral peptitle uyarılan lenfositlerde yapılan sitokin boncuk dizisi (CBA) analizleri, DA varlığında Th2 ağırlıklı bir yanıt yönelimi olduğunu göstermiştir ($p < 0,05$). Ayrıca floresan mikroskopi, polimorfonükleer lökositlerde forbol miristat asetat ile indüklenen NETozis üzerinde 30 U DA'nın baskılayıcı etkisini ortaya koymuştur. Genel olarak bu bulgular, DA'nın SARS-CoV-2 ile ilişkili yanıtları çoklu mekanizmalar üzerinden modüle edebileceğine dair ön ve hipotez oluşturucu kanıtlar sunmaktadır. Bu bulguların doğrulanması için daha büyük örneklemli ve yeterli istatistiksel güce sahip çalışmalara ihtiyaç vardır. Bununla birlikte klinik etkinlik ve olası profilaktik rolün ortaya konması, uygun şekilde tasarlanmış in vivo ve hasta temelli çalışmalarla doğrulanmayı gerektirmektedir.

Anahtar Kelimeler: *Koronavirüs hastalığı 2019, şiddetli akut solunum yolu sendromu koronavirüs 2, dornaz alfa, nötrofil ekstraselüler tuzakları.*

Recieved: 4.09.2025
Revised: 22.12.2025
Accepted: 8.02.2026

[*] ORCID: 0000-0003-4725-3200, Department of Biochemistry, Faculty of Pharmacy, Fenerbahçe University, Istanbul, Turkey; Acibadem Labcell Cellular Therapy Laboratory, Istanbul, Turkey
[**] ORCID: 0000-0002-4173-6634, Acibadem Labcell Cellular Therapy Laboratory, Istanbul, Turkey; Transgenic Cell Technologies and Epigenetic Application and Research Center (TRGENMER), Üsküdar University, Istanbul, Turkey; Molecular Biology and Genetics Department, Faculty of Engineering and Natural Science, Üsküdar University, Istanbul, Turkey
[***] ORCID: 0000-0001-5370-6865, Institute of Health and Science, Department of Medical Biotechnology, Acibadem Mehmet Ali Aydinlar University, Istanbul, Turkey
[****] ORCID: 0000-0002-6136-5033, Institute of Health and Science, Department of Medical Biochemistry, Acibadem Mehmet Ali Aydinlar University, Istanbul, Turkey
[*****] ORCID: 0000-0002-1293-9520, Acibadem Labcell Cellular Therapy Laboratory, Istanbul, Turkey; Institute of Health and Science, Department of Medical Biotechnology, Acibadem Mehmet Ali Aydinlar University, Istanbul, Turkey
[******] ORCID: 0000-0002-5988-5312, Acibadem Labcell Cellular Therapy Laboratory, Istanbul, Turkey; Institute of Health and Science, Department of Medical Biotechnology, Acibadem Mehmet Ali Aydinlar University, Istanbul, Turkey
[*******] ORCID: 0000-0003-2514-4142, Institute of Health and Science, Department of Biostatistics and Bioinformatics, Acibadem Mehmet Ali Aydinlar University, Istanbul, Turkey
[********] ORCID: 0000-0002-0682-5869, Acibadem Labcell Cellular Therapy Laboratory, Istanbul, Turkey
[*********] ORCID: 0000-0002-9269-8383, Acibadem Labcell Cellular Therapy Laboratory, Istanbul, Turkey; Institute of Health and Science, Department of Medical Biochemistry, Acibadem Mehmet Ali Aydinlar University, Istanbul, Turkey
[**********] ORCID: 0000-0003-3454-9870, Acibadem Labcell Cellular Therapy Laboratory, Istanbul, Turkey; Institute of Health and Science, Department of Medical Biotechnology, Acibadem Mehmet Ali Aydinlar University, Istanbul, Turkey; Acıbadem Altunizade Hospital, Department of Pediatric Hematology and Oncology, Istanbul, Turkey
[***********] ORCID: 0000-0002-9329-4698, Pharmaceutical Technology Department, Faculty of Pharmacy, Biruni University, Istanbul, Turkey
[************] ORCID: 0000-0002-4782-5355, Acibadem Labcell Cellular Therapy Laboratory, Istanbul, Turkey

[°] Corresponding Author; Derya DİLEK KANÇAĞI
E-mail: derya.kancagi@gmail.com

INTRODUCTION

The SARS-CoV-2 virus, which was first identified in Wuhan, China, in December 2019, has since spread worldwide and tragically resulted in the loss of over 5 million lives (Msemburi et al., 2023). This virus causes Coronavirus disease 2019 (COVID-19) disease, primarily affecting the human respiratory system and leading to severe pneumonia, coagulopathy, hyperinflammation, and acute respiratory distress syndrome (ARDS). The onset of SARS-CoV-2 infection involves the spike protein-mediated infection of respiratory cells and subsequent cytokine release reactions that contribute to ARDS development (Matthay et al., 2019). In this context, neutrophil activation has been implicated in the disease pathology, particularly in the development of ARDS (Barnes et al., 2020).

Neutrophils, apart from their role in engulfing microbes and releasing antimicrobial substances, are involved in the formation of neutrophil extracellular traps (NETs), reticulated extensions containing granular proteins and DNA strands (Brinkmann et al., 2004; Schönrich Raftery, 2016). While NETs play a crucial role in the immune response, they can also contribute to the pathogenesis of various diseases, especially viral infections, causing secondary damage (Schönrich Raftery, 2016).

Dornase alfa, a recombinantly produced enzyme known as deoxyribonuclease I (rhDNAase I), specifically breaks down DNA and has been successfully used to reduce lung fluid viscosity in patients with cystic fibrosis (Fitzgerald et al., 2005). Its use in combination with standard therapies has been shown to promote pulmonary function recovery in cystic fibrosis treatment (Yang Montgomery, 2021). Remarkably, dornase alfa has also demonstrated potential in treating ARDS (Morris Mullan, 2004). COVID-19 caused by SARS-CoV-2 may trigger a cytokine-storm–like response, leading to sepsis and severe, potentially fatal ARDS. Cystic fibrosis patients also show cytokine imbalance and hyperinflammatory profiles that resemble aspects of the COVID-19 disease process. This mechanistic overlap provides a rationale for translating evidence from cystic fibrosis/ARDS into SARS-CoV-2–related settings (Peckham et al., 2020). Notably, some clinical studies have observed a lower risk of severe disease in cystic fibrosis patients with SARS-CoV-2 infection, possibly attributed to the use of dornase alfa (Colombo et al., 2022). This observation has sparked initiatives exploring the use of dornase alfa in COVID-19 treatment, such as COVI-Dornase and COVASE (Desilles et al., 2020). Additionally, DNase1L3 has been considered for its potential in reducing vascular occlusion due to COVID-19 (Jiménez-Alcázar et al., 2017). Previous clinical studies have reported the promising effects of nebulized dornase alfa in reducing inflammation and oxygen requirements in hospitalized patients with COVID-19 pneumonia (Porter et al., 2024).

Similarly, in our preliminary report (Okur et al., 2020), we presented early invitro and limited invivo evidence (Vero/MDBK experiments and n=3 cases) regarding the potential effects of dornase alfa (DA) in SARSCoV2 infection.

Because DA is a DNase that targets extracellular DNA, its activity does not directly explain an effect on an RNA virus such as SARS-CoV-2. Accordingly, whether DA acts indirectly by altering NET/extracellular DNA–rich airway microenvironments, inflammatory responses, or virus–host interactions remains insufficiently defined. Building on this research line, the present study aimed to test mechanistic hypotheses by evaluating whether DA modulates SARS-CoV-2 in vitro through spike-associated viral entry/internalization, viral RNA integrity and infectivity, NETosis, and Th1/Th2 polarization.

MATERIALS AND METHODS

SARS-CoV-2 isolation

The study included nasopharyngeal and oropharyngeal cavity samples from four volunteers who tested positive for SARS-CoV-2 via RT-PCR in Acıbadem Healthcare Group hospitals. The isolation of SARS-

CoV-2 RNA from the collected patient samples followed previously described procedures (Sir Karakus et al., 2021; Taştan et al., 2020). In brief, the Vero cell line (CCL-81, ATCC, USA) was utilized for virus isolation and propagation. The virus culture initiation occurred in a 96-well plate and was subsequently scaled up in volume in a viral medium composed of high-glucose DMEM (Thermo Fisher Scientific Inc., USA), 2% fetal bovine serum (Thermo Fisher Scientific Inc., USA), and 1% penicillin-streptomycin-amphotericin (PSA) solution (Pan-Biotech GmbH, Aidenbach, Germany). The progression of virus replication and isolation was monitored by observing cytopathic effects during the propagation process. The supernatants obtained at the end of the production were pooled and concentrated 10–15 times (Sir Karakus et al., 2021). Unless otherwise stated, experiments were repeated in at least three independent biological replicates (≥3 separate experiments performed on different days/independent preparations). Within each independent experiment, conditions were run in technical triplicate (three replicate wells/measurements). For analysis and plotting, technical triplicates were averaged within each experiment, and summary statistics [mean ± standard deviation (SD)] were calculated across independent experiments.

Viral inactivation assay

Vero cells were seeded at 10,000 cells/well in flat-bottom 96-well plates with complete DMEM (10% FBS; 1% penicillin/streptomycin/amphotericin B) and incubated overnight at 37°C. SARS-CoV-2 (100× $TCID_{50}$; Taştan et al., 2020) was pre-incubated 1 h at RT with dornase alfa, then added to cells. Final concentrations were 3, 10, and 30 U/mL (i.e., 3, 10, 30 µg/mL given 1 mg/mL = 1000 U/mL). These levels were chosen a priori from published rhDNase I applications—where short ex vivo incubations at approximately 10 U have been reported—to span a sub-maximal activity range suitable for Vero cells while enabling dose–response assessment (Fisher et al., 2021). After 96 h, MTT (3-(4,5-dimethylthiazol-2-yl)-2,5-diphenyltetrazolium bromide) was performed per manufacturer; absorbance was read at 450 nm (FLUOstar Omega). Plate included mock, virus-only, and DA-only controls. Data were background-subtracted, normalized to mock, and reported as mean ± SD; % viability and % inactivation were calculated relative to virus-only.

QDot's production and characterization

Quantum Dots (QDots) are minute crystalline structures in the nanoscale, functioning as semiconductors with just a few atomic sizes, typically ranging between 2 and 10 nm, derived from compounds found within the periodic table's II-VI or III-V elements (Ozkan, 2004). Due to their small dimensions, both metallic and non-metallic QDots exhibit quantum effects, emitting narrow-band light in the ultraviolet (UV) region and displaying strong fluorescence and remarkable photostability (Kuang et al., 2011; Xu Chen, 2012). This makes QDots suitable for several applications (Maysinger et al., 2007; Singh Lillard, 2009; Xu Chen, 2012).

Production

QDots were synthesized using a microwave-assisted method. In brief, 0.5 g of p-phenylenediamine (Sigma Aldrich Chemie GmbH, Eschenstraße 5, 82024 Taufkirchen, Germany) served as a carbon source, and 1g of formamide (Sigma Aldrich Chemie GmbH, Eschenstraße 5, 82024 Taufkirchen, Germany) acted as a hetero atom. This mixture, combined with 15 ml of distilled water, was thoroughly mixed and transferred to the microwave reactor (Microwave 300, Anton Paar, St. Albans, Hertfordshire, AL4 0LA, UK). After the reaction, N-doped QDots were obtained, confirmed by UV light (365 nm), which revealed a red emission. The mixture was gently stirred overnight at room temperature. A final confirmation under UV light (365 nm) was performed before dialyzing the QDots.

Characterization

Analysis of physical appearances, particle size, and zeta potential of QDots has been conducted (Supplementary Figure 1 and Supplementary Table 1.). The determination of particle size and distribution was accomplished using Anton Paar Lite Sizer 500, with a sample size of n = 6 for particle size measurements and n = 12 for zeta potential measurements.

Quantum yield

The optical properties of QDots were assessed using a Spectrofluorometer (Model 229129, Agilent Technologies, 5301 Stevens Creek Blvd., Santa Clara, CA 95051, USA). QDots were excited, and their emitted light was recorded. The experimental procedure was adapted from the literature (Mirtchev et al., 2012). The quantum yield was calculated according to the well-established method outlined in the literature (Camlik et al., 2022).

Spike labeling with qdots assay and analysis of labelled spike protein blockage with dornase alfa

10,000 cells/well were seeded into a flat-bottom 96-well plate with complete DMEM (Wisent, Multicell 319-066-CL; 10% Fetal-Bovine Serum, 1% penicillin/streptomycin). S (spike) PepTivator, a collection of freeze-dried peptides encompassing the dominant sequence regions of the surface glycoprotein (also known as the spike protein or "S") of SARS-CoV-2 (GenBank MN908947.3, Protein QHD43416.1) (Miltenyi Biotech, GmbH, Bergisch Gladbach, Germany; cat# 130-126-700), was incubated with QDots E3 for 1 hour at 37°C a CO_2 incubator. After incubation, 3U, 10U, and 30U dornase alfa were added to the Spike-QDots mixture. Treated Spike-QDots- dornase alfa mixture was added onto Vero cells. After 48-hour incubation at 37°C a CO_2 incubator, spike cultivators were tracked by QDots labeling in APC-A750-A via flow cytometry (Buranda et al., 2011). Flow analysis was performed with the CYTOFLEX (Beckman Coulter, USA). Qdot fluorescence was also visualized macroscopically under UV/405 nm illumination.

q-RT-PCR assay

q-RT-PCR analyses were conducted using two different experimental setups for active virus in BSL-3 conditions. (1) Infected supernatants: RNA was extracted with Direct-zol and analyzed using DiaCarta QuantiVirus on LightCycler 96 (targets ORF1ab/N/E; triplicates; standard curve $R^2 \geq 0.99$, efficiency 90–110%). (2) Naked RNA ± DA: Purified SARS-CoV-2 RNA was incubated with DA (3/10/30 U/mL; [37°C], 30–60 min) vs. RNA-only, RNA+$MgSO_4$. SARS-CoV-2–specific qRT-PCR was performed with the QuantiVirus SARS-CoV-2 Test Kit (DiaCarta) on a Roche LightCycler 96, following the manufacturer's instructions (Targets: ORF1ab, N, and E; kit-specific panels). Each sample was run in technical triplicate; no-template controls (NTC) and positive controls were included on every plate.

Sequencing

Whole-genome sequencing (WGS) was performed on live viral RNA after 100× $TCID_{50}$ SARS-CoV-2 had been pre-incubated for 1 h with dornase alfa (3, 10, or 30 U/mL) or buffer only (no DA). Then the samples were analyzed via whole-genome analysis. The quality controls of the raw data generated by the reading were carried out with the FastQC tool. The raw data obtained were first trimmed to certain lengths using cutadapt (v3.2) and fgbio tools, considering the quality parameters of the 5' and 3' ends and the primers used. It was then aligned against the reference genome (NCBI Reference Sequence: NC_045512.2) using the BWA (v.0.7.12) tool. The GATK v.4 tool was used for alignment corrections in Indel regions, normalization of DNA sequence quality values, and variant extraction. All obtained variants were visually checked with the GenomeBrowse (Golden Helix) tool. Then, the annotation of the variants was completed with the Variant Effect Predictor program.

Cytokine bead array

Peripheral blood mononuclear cells (PBMCs) were isolated from a healthy volunteer using Ficoll-paque plus overlay (GE Healthcare, Chalfont St Giles, UK).

Subsequently, 10,000 PBMCs per well were seeded in a 96-U bottom well plate with complete DMEM (containing 10% Fetal Bovine Serum, 1% penicillin/streptomycin). The cells were treated with a mix of spike (S), nucleocapsid (N), and membrane (M) PepTivator (Miltenyi Biotec, GmbH, Bergisch Gladbach, Germany), with 20 µL added to each well. Following this, they were incubated with 3U and 10U of dornase alfa, along with 420 µg/mL $MgSO_4$, for 72 hours in a humidified 37°C CO_2 incubator. After the incubation period, a Cytometric Bead Assay was conducted using a MACSPLEX Cytokine 10 kit (Miltenyi Biotec, GmbH, Bergisch Gladbach, Germany), following the manufacturer's protocol, on the supernatant from the cell suspension. Flow analysis of the samples was performed using the MACSQUANT Analyzer (Miltenyi Biotec, GmbH, Bergisch Gladbach, Germany) (Sir Karakus et al., 2021; Turan et al., 2021).

Clearance of NET formation by dornase alfa

PBMCs obtained as described previously were seeded on a 24-well plate with $1x10^6$ /well concentration in complete medium (RPMI enriched with 10% Fetal-Bovine Serum, 1% penicillin/streptomycin). As previously described in the literature, the culture was supplemented with 700 nM phorbol myristate acetate (PMA) for NET formation (Hoppenbrouwers et al., 2017). Then, the culture treated with 420 µg/mL $MgSO_4$ and 0, 3U, 10U, and 30U Dornase Alfa was incubated for 24 hours. After incubation, the wells were stained with DAPI (Sigma Aldrich, USA), and NET formation was examined under a fluorescent microscope (ZEISS Axio Vert.A1). PBMCs were assessed under unstimulated and PMA-stimulated conditions. DA + PMA was compared against PMA-only to evaluate changes consistent with NETosis suppression. No DA-only, heat-inactivated DNase, vehicle/buffer-only, or inhibitor controls were performed in this study.

Statistics

Student's t-tests were employed to assess normally distributed data presented on bar graphs, while the Mann-Whitney U test was utilized for comparing two groups of non-normally distributed data. Statistical analyses were conducted using both Graphpad Prism (trial version) and SPSS Statistics software. Each data point corresponds to an independent measurement and represents one of at least 3 separate experiments undertaken in triplicate, with the bar graph illustrating the mean and standard deviation of the mean. A significance threshold of $*p < 0.05$ was applied to all tests, with "ns" indicating non-significance.

RESULTS AND DISCUSSIONS

Role of dornase alfa in the blockade of SARS-CoV-2 infectivity

Cytotoxic effect of dornase alfa on the virus

In the MTT assay, dornase alfa treatment increased Vero cell viability after SARS-CoV-2 exposure. Although 10 U and 30 U showed higher viability than the virus-only control, the difference reached statistical significance only for 30 U ($p = 0.0172$) (Figure 1.).

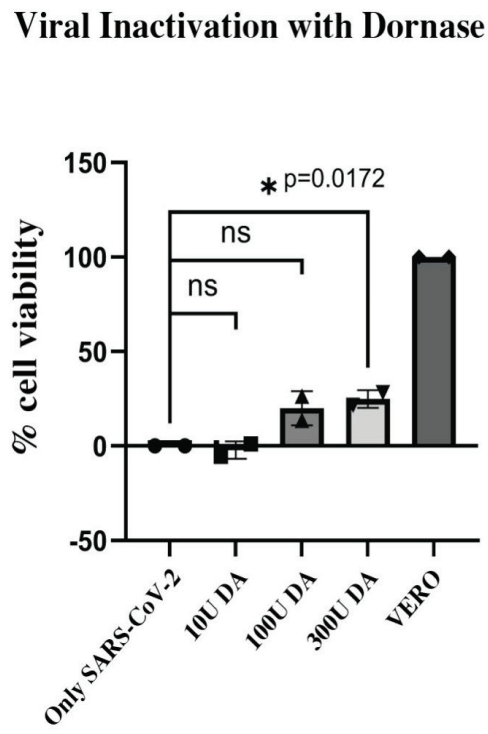

Figure 1. Vero cells were exposed to SARS-CoV-2 (100×$TCID_{50}$) pre-incubated with increasing concentrations of dornase alfa (DA). DA at 30 U significantly improved cell viability compared with the virus-only control. Cell viability (%) was quantified using a colorimetric ELISA-based assay. Each data point represents one independent biological replicate (one of ≥3 separate experiments from pooled virus), with each experiment performed in technical triplicate. Bars show the mean ± SD across independent experiments. Statistical significance was assessed using an unpaired two-tailed Student's t-test or Mann–Whitney U test, as appropriate ($p < 0.05$).

Effect of dornase alfa on SARS-CoV-2 neutralization: spike blocking analysis

Docking analyses suggested favorable binding between dornase alfa and the SARS-CoV-2 spike protein. Guided by this result, we evaluated whether dornase alfa affects spike availability using Qdot-labeled spike protein. Increasing dornase alfa concentrations produced a dose-dependent reduction in Qdot signal, with significant effects at 10 U ($p = 0.0122$) and 30 U ($p < 0.0001$) (Figure 2.).

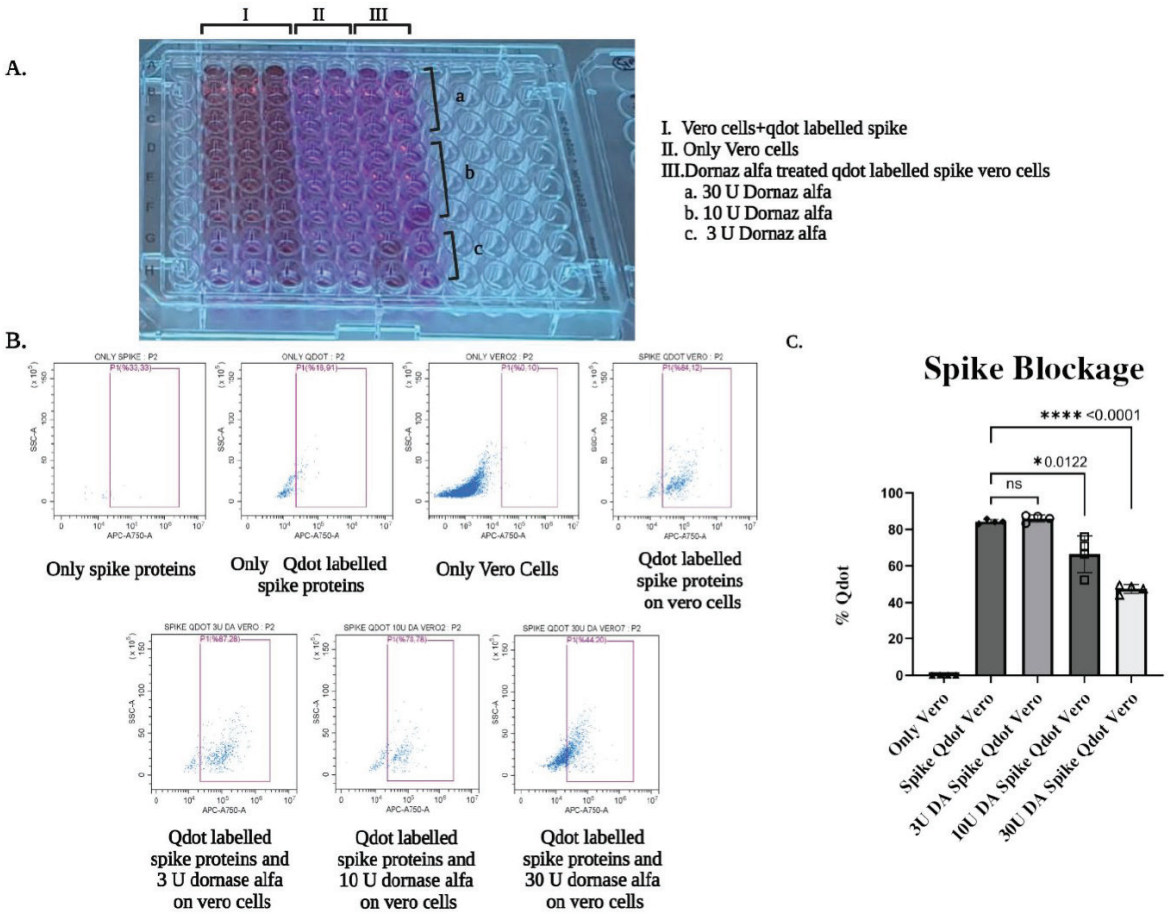

Figure 2. A. Macroscopic luminescence view of the plate under UV light. **B.** Plots show the amount of spike protein detected by flow cytometry after treatment with different concentrations of dornase alfa. A statistically significant neutralization of viral spike proteins has been detected, particularly in response to the use of 10U and 30U dornase alfa. **C.** The graph shows the mean fluorescence intensity (MFI) of Qdot signals across replicates. Each data point represents one independent biological replicate (one of ≥3 separate experiments from pooled virus), with each experiment performed in technical triplicate. Bars show the mean ± SD across independent experiments. Statistical significance was assessed using an unpaired two-tailed Student's t-test or Mann–Whitney U test, as appropriate ($p < 0.05$).

Effect of dornase alfa on naked SARS-CoV-2 RNA copy number: qRT-PCR analysis

Significant changes in viral copy numbers of isolated SARS-CoV-2 RNA were observed following treatment with different amounts of dornase alfa (p= 0.0163 for all concentrations). These changes in viral copy numbers due to dornase alfa usage were statistically significant (Figure 3.).

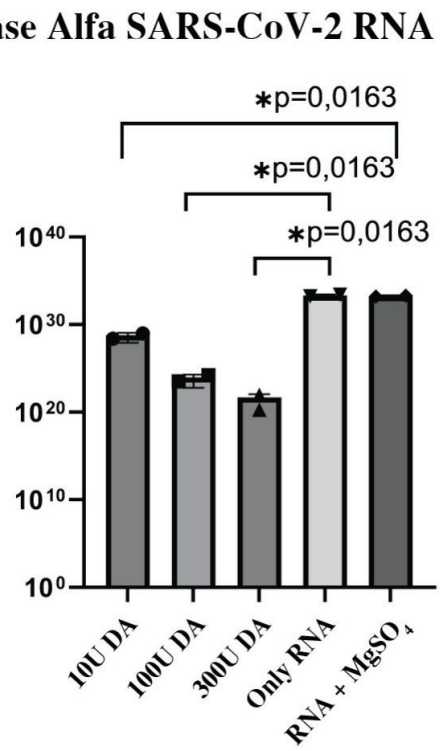

Figure 3. Purified ("naked") SARS-CoV-2 RNA was incubated with increasing concentrations of dornase alfa, and viral RNA levels were quantified by SARS-CoV-2–specific qRT-PCR. Viral copies/mL were calculated from a standard curve. Bars show viral copy number per mL for each condition (p values indicated). Each data point represents one independent biological replicate (one of ≥3 separate experiments from pooled virus), with each experiment performed in technical triplicate. Bars show the mean ± SD across independent experiments. Statistical significance was assessed using an unpaired two-tailed Student's t-test or Mann–Whitney U test, as appropriate ($p < 0.05$).

Effect of Dornase alfa on naked SARS-CoV-2 RNA sequence: Whole genome sequencing

Whole genome sequencing analysis was conducted to investigate potential changes in the genome sequence of the SARS-CoV-2 virus incubated with various concentrations of dornase alfa. Results revealed no significant difference between viral RNA left untreated and viral RNA treated with 3U and 10U dornase alfa (high coverage). However, viral RNA treated with 30U of dornase alfa exhibited poor quality, and whole genome sequencing was not feasible (low coverage level) (Supplementary Figure 2.). A minimum threshold of 100 depth was established for consensus fastas, with a mean depth >10000.

RNA copy number isolated from dornase alfa-treated SARS-CoV-2: qRT-PCR analysis

Evaluation of the effect of dornase alfa directly incubated with SARS-CoV-2 demonstrated no significant change in viral copy numbers (Figure 4.).

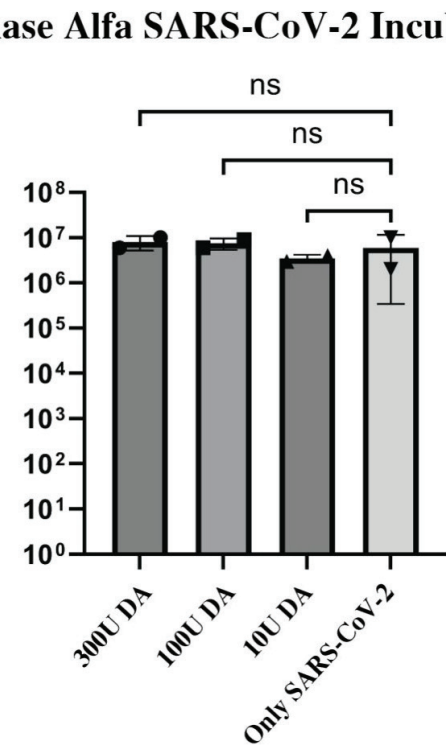

Figure 4. Following pre-incubation of SARS-CoV-2 (100×$TCID_{50}$) with increasing concentrations of dornase alfa, viral RNA was extracted and quantified by SARS-CoV-2–specific qRT-PCR. Viral copies/mL were calculated from a standard curve. Bars show viral copy number per mL for each condition. Each data point represents one independent biological replicate (one of ≥3 separate experiments from pooled virus), with each experiment performed in technical triplicate. Bars show the mean ± SD across independent experiments. Statistical significance was assessed using an unpaired two-tailed Student's t-test or Mann–Whitney U test, as appropriate ($p < 0.05$).

Effect of dornase alfa on the immune cytokine response due to the SARS-CoV-2 infection

Effect of dornase alfa on Th2 immunological response: Cytokine bead array analysis

PBMCs from two donors were stimulated with spike protein pre-incubated with dornase alfa, and cytokine responses were quantified by CBA. Dornase alfa shifted the response toward a Th2-skewed profile, with significant changes at 3 U in the IL-17/IL-10, TNF-α/IL-6, and IFN-γ/IL-6 ratios (p = 0.0095, p = 0.0198, and p = 0.0316, respectively). At 10 U, IFN-γ/IL-6 and TNF-α/IL-6 ratios also differed significantly compared with PBMC-only controls (p = 0.0358 and p = 0.0298, respectively) (Figure 5; Supplementary Table 2.).

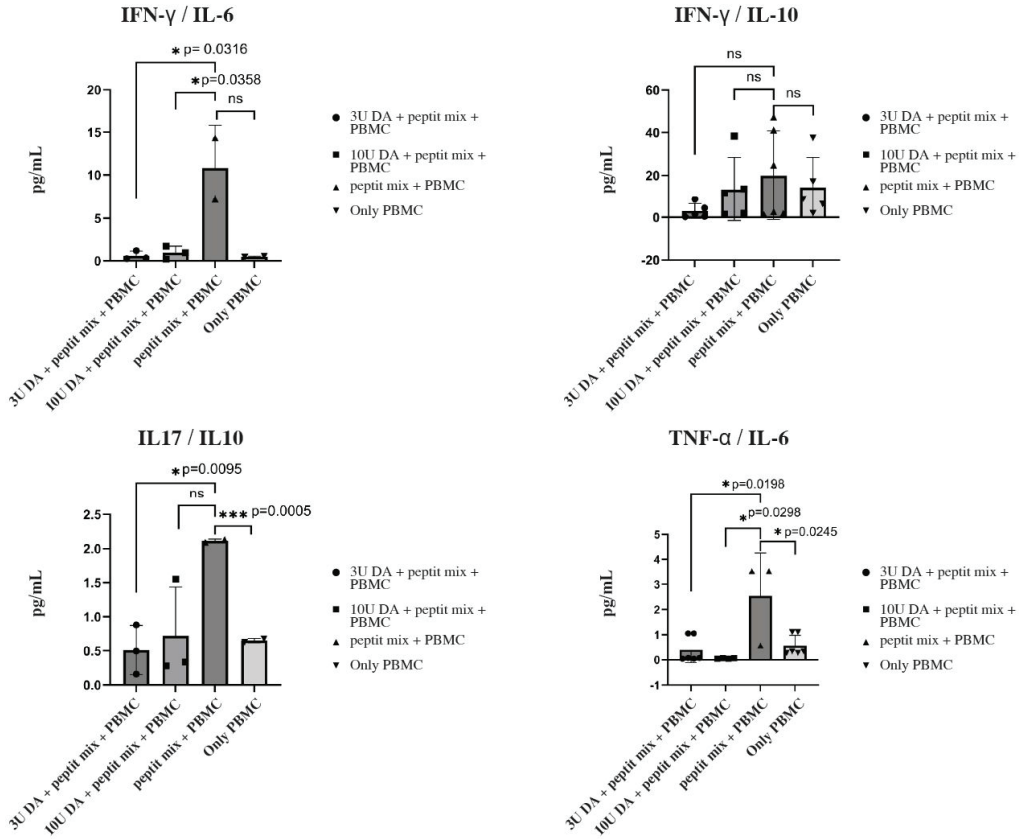

Figure 5. The immune response in PBMC cells treated with different concentrations of dornase alfa and viral peptide mix was examined by CBA assay after 72h. The bar charts indicate the ratio of Th1 response to Th2 response. Only PBMC: Negative Control; Peptide Mix + PBMC: Positive Control. Each data point represents one independent biological replicate (one of ≥3 separate experiments from pooled virus), with each experiment performed in technical triplicate. Bars show the mean ± SD across independent experiments. Statistical significance was assessed using an unpaired two-tailed Student's t-test (normal data) or Mann–Whitney U test (non-normal data), as indicated; $p < 0.05$ was considered significant.

NET formation with dornase alfa: Fluorescent microscopy analysis

To assess the impact of dornase alfa on NETs induced by PMA, NETs were treated with different concentrations of dornase alfa for 24 hours and stained with DAPI dye. Results indicated that virus pathophysiology was altered by 3U, 10U, and 30U dornase alfa (Figure 6.).

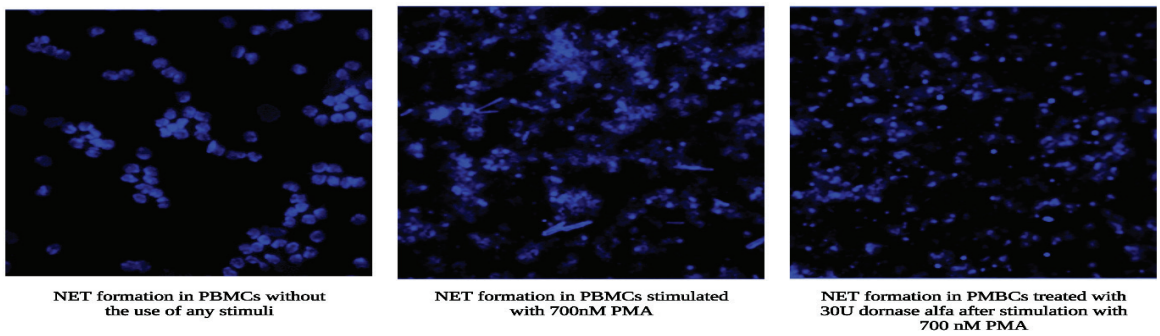

Figure 6. Image of NET formation in PBMC cells stained with DAPI dye under fluorescence microscopy**.**

CONCLUSION

Clinical studies have suggested that dornase alfa may benefit patients with SARS-CoV-2–related ARDS, reporting improvements in oxygenation, clinical status, and time to discharge (Desilles et al., 2020; Turan et al., 2021; Porter et al., 2024). In addition, Colombo et al. observed lower COVID-19 severity among cystic fibrosis patients receiving dornase alfa as part of standard care (Colombo et al., 2022). Building on these clinical observations, we sought to explore potential mechanisms by examining DA-driven immune modulation and its effects on viral components.

In our in vitro system, dornase alfa (DA; 10–30 U/mL) was associated with reduced SARS-CoV-2–induced cytopathic effects, potentially through two non-exclusive mechanisms: interference with spike-mediated entry and effects detected on purified ("naked") viral RNA. Qdot-based readouts supported a DA-dependent interaction with spike/entry processes, and pre-incubation of purified SARS-CoV-2 RNA with DA was associated with reduced qRT-PCR–derived copy number. In contrast, no copy-number reduction was observed when intact virions were incubated with DA before RNA extraction and qRT-PCR, which is biologically plausible given that the genome is shielded by the nucleocapsid and viral envelope. Importantly, DA is a DNase rather than an RNase; therefore, the "naked RNA" signal should be interpreted cautiously as hypothesis-generating only and may reflect indirect or matrix-related effects (e.g., carryover DNA, divalent cation–dependent assay effects, or other reaction-condition artifacts) rather than direct RNA cleavage. Accordingly, we do not interpret this observation as evidence of RNase-like activity, but as an indirect readout that requires orthogonal validation. Overall, these findings support biological plausibility for DA affecting entry-adjacent steps while cautioning against over-interpreting the "naked RNA" observation as RNase-like activity. A prior docking study is consistent with potential DA–spike interaction (Salman et al., 2020). Furthermore, Qdot-based quantitative flow cytometry showed a dose-dependent decrease in fluorescence with increasing dornase alfa, consistent with DA–spike interaction and reduced viral internalization as a surrogate measure of entry. These data do not directly quantify infectivity, which was assessed separately in the functional assays. Importantly, DA is a recombinant human DNase I and is not established as an RNase; therefore, the apparent "naked RNA" signal should be interpreted cautiously as hypothesis-generating and may reflect indirect or matrix-related effects rather than direct RNA cleavage. Under specific experimental conditions, DNA-mediated catalysis against RNA substrates has been described (e.g., DNAzymes) (Glick et al., 2014), and RNA digestion by other DNases has been reported in non-neutral environments (e.g., DNase II under mildly acidic conditions) (Zhuang et al., 2024). Accordingly, in complex mixtures where DNA and RNA co-exist, matrix effects—including potential contributions from cell-derived DNA fragments—could influence RNA integrity readouts. Orthogonal validation (e.g., RNase-inhibitor controls, heat-inactivated DA, and assays that discriminate true RNA cleavage from artifacts) will be required to resolve this mechanism. Early COVID-19 studies described a cytokine-storm phenotype with dysregulated T-cell immunity and broad shifts in inflammatory mediators; Guo et al. similarly reported widespread cytokine increases in patients, including IL-1β, IL-6, IL-8, IL-17, IFN-γ, and IL-10 (Guo et al., 2021). In this context,

our spike-stimulated PBMC data suggest that dornase alfa (DA) may modulate T-helper polarization toward a Th2-skewed profile, a concept that has been discussed as potentially relevant when effective antivirals are limited (Mamber et al., 2020). However, these observations are exploratory, derived from an in vitro system with a small donor number, and do not establish clinical benefit; validation in larger, longitudinal in vivo studies will be required (Gupta et al., 2022). Beyond cytokine dysregulation, NET formation has been implicated in ARDS and SARS-CoV-2 morbidity, and our microscopy-based readouts are consistent with a DNA/NET-directed effect of DA (Toma et al., 2021; Weber et al., 2020), aligning with ex vivo evidence of rapid NET dissolution in COVID-19 sputum after DNase I treatment (Fisher et al., 2021); nevertheless, these findings remain hypothesis-generating and require rigorous in vivo confirmation.

In this in vitro model, dornase alfa (DA) reduced assay-measured viral infectivity, decreased spike-associated viral internalization, and modulated inflammatory readouts, including a Th2-skewed response, while attenuating PMA-induced NETosis. Together with the hypothesis-generating observations reported by Okur et al. (2020), these results provide a preliminary mechanistic rationale to further investigate DA in the context of SARS-CoV-2 infection. However, given the limited sample size (n=3) and potential donor-to-donor variability despite harmonized procedures, statistical power is constrained, and the findings should be interpreted cautiously. Accordingly, this work should be considered preliminary and hypothesis-generating, and it requires validation in appropriately designed in vivo models and patient-based studies before any conclusions can be drawn regarding clinical efficacy or prophylactic use. In addition, further confirmatory experiments were beyond the scope of the present study due to laboratory and biosafety constraints and limited access to live virus materials. Future studies with larger sample sizes and independent replication will be essential to confirm and extend these findings.

ACKNOWLEDGEMENTS

The author(s) received no financial support for the research. The authors thank Acibadem Labcell Cellular Therapy Center for their support of the project.

ETHICS COMMITTEE APPROVAL

An informed consent form was obtained from the patients participating in the study (Ethics Committee Approval: Acıbadem Mehmet Ali Aydınlar University, number: 2020-06/03).

AUTHOR CONTRIBUTION STATEMENT

D.D.K., C.T., K.B.K., S.A., D.Ç., Y.B., G.S.K. and B.Y. designed, completed, and/or analyzed preclinical experiments. S.A. analyzed SARS-CoV-2 sequencing results. I.T.D. performed qdot production and its quality control analysis. D.D.K., C.T., K.B.K, Y.B. K.Y. and İ.T.D. wrote the manuscript. E.O. led the investigation and development project and contributed to the design and interpretation of the data. All authors contributed to the editing of the manuscript and approved the final version.

CONFLICTS OF INTEREST

The authors declare that there is no conflict of interest.

REFERENCES

Barnes, B. J., Adrover, J. M., Baxter-Stoltzfus, A., Borczuk, A., Cools-Lartigue, J., Crawford, J. M., ... Egeblad, M. (2020). Targeting potential drivers of COVID-19: Neutrophil extracellular traps. *Journal of Experimental Medicine*, *217*(6), e20200652. https://doi.org/10.1084/jem.20200652

Brinkmann, V., Reichard, U., Goosmann, C., Fauler, B., Uhlemann, Y., Weiss, D. S., ... Zychlinsky, A. (2004). Neutrophil extracellular traps kill bacteria. *Science*, *303*(5663), 1532-1535. https://doi.org/10.1126/science.1092385

Buranda, T., Wu, Y., Sklar, L. A. (2010). Quantum dots for quantitative flow cytometry. In *Flow Cytometry Protocols* (pp. 67-84). Totowa, NJ: Humana Press. https://doi.org/10.1007/978-1-61737-950-5_4

Camlik, G., Ozakca, I., Bilakaya, B., Ozcelikay, A. T., Velaro, A. J., Wasnik, S., Degim, I. T. (2022). Development of composite carbon quantum dots-insulin formulation for oral administration. *Journal of drug delivery science and technology*, *76*, 103833. https://doi.org/10.1016/j.jddst.2022.103833

Colombo, C., Cipolli, M., Daccò, V., Medino, P., Alghisi, F., Ambroni, M., ... Alicandro, G. (2022). Clinical course and risk factors for severe COVID-19 among Italian patients with cystic fibrosis: a study within the Italian Cystic Fibrosis Society. *Infection*, *50*(3), 671-679. https://doi.org/10.1007/s15010-022-01779-6

Desilles, J. P., Gregoire, C., Le Cossec, C., Lambert, J., Mophawe, O., Losser, M. R., ... Pottecher, J. (2020). Efficacy and safety of aerosolized intra-tracheal dornase alfa administration in patients with SARS-CoV-2-induced acute respiratory distress syndrome (ARDS): a structured summary of a study protocol for a randomised controlled trial. *Trials*, *21*(1), 548. https://doi.org/10.1186/s13063-020-04540-y

Fisher, J., Mohanty, T., Karlsson, C. A., Khademi, S. H., Malmström, E., Frigyesi, A., ... Linder, A. (2021). Proteome profiling of recombinant DNase therapy in reducing NETs and aiding recovery in COVID-19 patients. *Molecular Cellular Proteomics*, *20*, 100113. https://doi.org/10.1016/j.mcpro.2021.100113

Fitzgerald, D. A., Hilton, J., Jepson, B., Smith, L. (2005). A crossover, randomized, controlled trial of dornase alfa before versus after physiotherapy in cystic fibrosis. *Pediatrics*, *116*(4), e549-e554. https://doi.org/10.1542/peds.2005-0308

Glick, B. R., Patten, C. L., Delovitch, T. L. (Eds.). (2014). *Medical biotechnology*. John Wiley Sons.

Guo, J., Wang, S., Xia, H., Shi, D., Chen, Y., Zheng, S., ... Li, L. (2021). Cytokine signature associated with disease severity in COVID-19. *Frontiers in immunology*, *12*, 681516. https://doi.org/10.3389/fimmu.2021.681516

Gupta, G., Shareef, I., Tomar, S., Kumar, M. S. N., Pandey, S., Sarda, R., ... Sinha, S. (2022). Th1/Th2/Th17 cytokine profile among different stages of COVID-19 infection. *National Academy Science Letters*, *45*(4), 363-369. https://doi.org/10.1007/s40009-022-01123-9

Hoppenbrouwers, T., Autar, A. S., Sultan, A. R., Abraham, T. E., van Cappellen, W. A., Houtsmuller, A. B., ... de Maat, M. P. (2017). In vitro induction of NETosis: Comprehensive live imaging comparison and systematic review. *PloS one*, *12*(5), e0176472. https://doi.org/10.1371/journal.pone.0176472

Jiménez-Alcázar, M., Rangaswamy, C., Panda, R., Bitterling, J., Simsek, Y. J., Long, A. T., ... Fuchs, T. A. (2017). Host DNases prevent vascular occlusion by neutrophil extracellular traps. *Science*, *358*(6367), 1202-1206. https://doi.org/10.1126/science.aam8897

Kuang, H., Zhao, Y., Ma, W., Xu, L., Wang, L., Xu, C. (2011). Recent developments in analytical applications of quantum dots. *TrAC trends in analytical chemistry*, *30*(10), 1620-1636. https://doi.org/10.1016/j.trac.2011.04.022

Mamber, S. W., Krakowka, S., Osborn, J., Saberski, L., Rhodes, R. G., Dahlberg, A. E., ... McMichael, J. (2020). Can unconventional immunomodulatory agents help alleviate COVID-19 symptoms and severity? *MSphere*, *5*(3), 10-1128. https://doi.org/10.1128/mSphere.00288-20

Matthay, M. A., Zemans, R. L., Zimmerman, G. A., Arabi, Y. M., Beitler, J. R., Mercat, A., ... Calfee, C. S. (2019). Acute respiratory distress syndrome. *Nature reviews Disease primers*, *5*(1), 18. https://doi.org/10.1038/s41572-019-0069-0

Maysinger, D., Behrendt, M., Lalancette-Hébert, M., Kriz, J. (2007). Real-time imaging of astrocyte response to quantum dots: in vivo screening model system for biocompatibility of nanoparticles. *Nano Letters*, *7*(8), 2513-2520. https://doi.org/10.1021/nl071611t

Mirtchev, P., Henderson, E. J., Soheilnia, N., Yip, C. M., Ozin, G. A. (2012). Solution phase synthesis of carbon quantum dots as sensitizers for nanocrystalline TiO 2 solar cells. *Journal of Materials Chemistry*, *22*(4), 1265-1269. https://doi.org/10.1039/C1JM14219A

Morris, C., Mullan, B. (2004). Use of dornase alfa in the management of ARDS. *Anaesthesia*, *59*(12), 1249-1249. https://doi.org/10.1111/j.1365-2044.2004.04018.x

Msemburi, W., Karlinsky, A., Knutson, V., Aleshin-Guendel, S., Chatterji, S., Wakefield, J. (2023). The WHO estimates of excess mortality associated with the COVID-19 pandemic. *Nature*, *613*(7942), 130-137. https://doi.org/10.1038/s41586-022-05522-2

Okur, H. K., Yalcin, K., Tastan, C., Demir, S., Yurtsever, B., Karakus, G. S., ... Ovali, E. (2020). Preliminary report of in vitro and in vivo effectiveness of dornase alfa on SARS-CoV-2 infection. *New microbes and new infections*, *37*, 100756. https://doi.org/10.1016/j.nmni.2020.100756

Ozkan, M. (2004). Quantum dots and other nanoparticles: what can they offer to drug discovery? *Drug Discovery Today*, *9*(24), 1065-1071. https://doi.org/10.1016/s1359-6446(04)03291-x

Peckham, D., McDermott, M. F., Savic, S., Mehta, A. (2020). COVID-19 meets Cystic Fibrosis: for better or worse? *Genes Immunity*, *21*(4), 260-262. https://doi.org/10.1038/s41435-020-0103-y

Porter, J. C., Inshaw, J., Solis, V. J., Denneny, E., Evans, R., Temkin, M. I., ... Papayannopoulos, V. (2024). Anti-inflammatory therapy with nebulized dornase alfa for severe COVID-19 pneumonia: a randomized unblinded trial. *Elife*, *12*, RP87030. https://doi.org/10.7554/eLife.87030.4

Xu, L., Chen, C. (2012). Physiological behavior of quantum dots. *Wiley Interdisciplinary Reviews: Nanomedicine and Nanobiotechnology*, *4*(6), 620-637. https://doi.org/10.1002/wnan.1187

Salman, S., Shah, F. H., Chaudhry, M., Tariq, M., Akbar, M. Y., Adnan, M. (2020). In silico analysis of protein/peptide-based inhalers against SARS-CoV-2. *Future Virology*, *15*(9), 557-564. https://doi.org/10.2217/fvl-2020-0119

Schönrich, G., Raftery, M. J. (2016). Neutrophil extracellular traps go viral. *Frontiers in immunology*, *7*, 366. https://doi.org/10.3389/fimmu.2016.00366

Singh, R., Lillard Jr, J. W. (2009). Nanoparticle-based targeted drug delivery. *Experimental and molecular pathology*, *86*(3), 215-223. https://doi.org/10.1016/j.yexmp.2008.12.004

Sir Karakus, G., Tastan, C., Dilek Kancagi, D., Yurtsever, B., Tumentemur, G., Demir, S., ... Ovali, E. (2021). Preclinical efficacy and safety analysis of gamma-irradiated inactivated SARS-CoV-2 vaccine candidates. *Scientific reports*, *11*(1), 5804. https://doi.org/10.1038/s41598-021-83930-6

Taştan, C., Yurtsever, B., Karakuş, G., Kançağı, D. D., Demir, S., Abanuz, S., ... Kocagöz, A. S. (2020). SARS-CoV-2 isolation and propagation from Turkish COVID-19 patients. *Turkish Journal of Biology*, *44*(7), 192-202. https://doi.org/10.3906/biy-2004-115

Toma, A., Darwish, C., Taylor, M., Harlacher, J., Darwish, R. (2021). The use of dornase alfa in the management of COVID-19-associated adult respiratory distress syndrome. *Critical care research and practice*, *2021*(1), 8881115. https://doi.org/10.1155/2021/8881115

Turan, R. D., Tastan, C., Dilek Kancagi, D., Yurtsever, B., Sir Karakus, G., Ozer, S., ... Ovali, E. (2021). Gamma-irradiated SARS-CoV-2 vaccine candidate, OZG-38.61. 3, confers protection from SARS-CoV-2 challenge in human ACEII-transgenic mice. *Scientific reports*, *11*(1), 15799. https://doi.org/10.1038/s41598-021-95176-2

Weber, A. G., Chau, A. S., Egeblad, M., Barnes, B. J., Janowitz, T. (2020). Nebulized in-line endotracheal dornase alfa and albuterol administered to mechanically ventilated COVID-19 patients: a case series. *Molecular Medicine*, *26*(1), 91. https://doi.org/10.1186/s10020-020-00206-6

Yang, C., Montgomery, M. (2021). Dornase alfa for cystic fibrosis. *Cochrane Database of Systematic Reviews*, (3). https://doi.org/10.1002/14651858.CD001127.pub5

Zhuang, J., Du, X., Liu, K., Hao, J., Wang, H., An, R., Liang, X. (2024). DNase II Can Efficiently Digest RNA and Needs to Be Redefined as a Nuclease. *Cells*, *13*(18), 1525. https://doi.org/10.3390/cells13181525